jove

Spatio-Temporal *In Vivo* Imaging of Ocular Drug Delivery Systems using Fiberoptic Confocal Laser Microendoscopy

Su Yin Chaw[1,2], **Tina Tzee Ling Wong**[3,4], **Subbu Venkatraman**[2,5], **Ann-Marie Chacko**[1]

[1] Laboratory for Translational and Molecular Imaging, Cancer and Stem Cell Biology Programme, Duke-NUS Medical School [2] School of Materials Science and Engineering, Nanyang Technological University [3] Singapore National Eye Centre [4] Singapore Eye Research Institute [5] Material Science & Engineering, National University of Singapore

Corresponding Author

Ann-Marie Chacko
gmsac@nus.edu.sg

Citation

Chaw, S.Y., Wong, T.T.L., Venkatraman, S., Chacko, A.M. Spatio-Temporal *In Vivo* Imaging of Ocular Drug Delivery Systems using Fiberoptic Confocal Laser Microendoscopy. *J. Vis. Exp.* (175), e62685, doi:10.3791/62685 (2021).

Date Published

September 27, 2021

DOI

10.3791/62685

URL

jove.com/video/62685

Abstract

Subconjunctival injection is an attractive route to administer ocular drugs due to easy trans-scleral access that bypasses anterior ocular barriers, such as the cornea and conjunctiva. While therapeutic effects and pharmacokinetics of the drugs upon subconjunctival injection have been described in some studies, very few assess the ocular distribution of drugs or drug delivery systems (DDS). The latter is critical for the optimization of intraocular DDS design and drug bioavailability to achieve the desired ocular localization and duration of action (e.g., acute versus. prolonged). This study establishes the use of fiberoptic confocal laser microendoscopy (CLM) to qualitatively study the ocular distribution of fluorescent liposomes in real-time in live mice after sub-conjunctival injection. Being designed for *in vivo* visual inspection of tissues at the microscopic level, this is also the first full description of the CLM imaging method to study spatio-temporal distribution of injectables in the eye after subconjunctival injection.

Introduction

The blood clearance, tissue distribution, and target occupancy of drugs in living systems are pillars to understanding *in vivo* drug disposition. In preclinical animal models, these parameters are typically assessed by frequent blood and tissue sampling at particular time points post drug administration. However, these procedures are generally invasive, often include non-survival measurements, and necessitate large animal cohorts for statistical powering. There might be extra cost and time incurred, along with ethical concerns for excessive use of animals. As a result, non-invasive imaging is fast becoming an integral step in biodistributions studies. Confocal laser microendoscopy (CLM[1,2]) is well-suited for ocular applications to non-invasively image the spatio-

temporal distribution of therapeutics in the eyes of live animals with high sensitivity and high resolution[1,3,4].

CLM has the potential to facilitate robust screening of ocular drug delivery systems (DDS), such as liposomes, prior to comprehensive quantification of the DDS and drug bioavailability. Liposomes are attractive for their flexibility in tuning their physicochemical and biophysical properties[5,6,7,8,9,10,11] to encapsulate a large variety of therapeutic cargo and control the tissue site of drug release and duration of action. Liposomes have been used in ocular applications for the delivery of large molecules, such as the monoclonal antibody bevacizumab[12], and small molecules like cyclosporine[13] and ganciclovir[14]. Drug-loaded liposomes have longer biological half-lives and prolonged therapeutic effects compared to non-liposomal "free drug" formulations. However, drug distribution in ocular tissue is typically extrapolated from drug concentrations in fluid components of the eye (i.e., blood, aqueous humor, and vitreous humor[15,16,17]). As the initial *in vivo* fate of the loaded drug cargo is defined by the properties of the nanocarrier itself, CLM imaging of the fluorescent liposomes can serve as a surrogate for the drug to reveal tissue targeting and *in situ* tissue residence times. Furthermore, visual evidence of delivery with CLM can steer DDS re-design, evaluate therapeutic benefits of the drug, and perhaps even predict adverse biological events (e.g., tissue toxicity due to undesirable localization of DDS for protracted periods of time).

Herein, a step-by-step procedure is detailed on how to study the ocular biodistribution of liposomes in live mice with a dual-band CLM system. This specific CLM system can detect two-color fluorescence (with green and red excitation lasers at 488 nm and 660 nm) in real-time, with a frequency of 8 frames/s. By physically placing the detection probe on the eye, the protocol demonstrates image acquisition and analysis of green-fluorescent liposomes upon subconjunctival administration in mice pre-injected intravenously (IV) with 2% Evans Blue (EB) dye. EB dye helps visualize the vascularized structures in the red fluorescence channel. We show representative results from a study assessing 100 nm neutral liposomes composed of the phospholipid POPC (i.e., 1-palmitoyl-2-oleoyl-glycero-3-phosphocholine) and doped with fluorescein-tagged phospholipid Fl-DHPE (i.e., *N*-(fluorescein-5-thiocarbamoyl)-1,2-dihexa-decanoylsn-glycero-3-phosphoethanolamine) at a ratio of 95% POPC: 5% Fl-DHPE (**Figure 1B**). CLM is able to capture the green fluorescein-tagged liposomes at 15 µm axial and 3.30 µm lateral resolution by delineation of EB-stained ocular tissue boundaries.

Protocol

All methods described here have been approved by the Institutional Animal Care and Use Committee (IACUC) at SingHealth (Singapore). Female C57BL/6 J mice (6- 8 weeks old; 18-20 g) were obtained from InVivos, Singapore, and housed in a temperature and light-controlled vivarium of Duke-NUS Medical School, Singapore. Animals were treated in accordance with the guidelines from the Association for Research in Vision and Ophthalmology (ARVO) statement for the use of animals in ophthalmic and vision research.

NOTE: A flow chart highlighting the main procedures is shown in **Figure 2**.

1. Preparation of contrast agents: Evans Blue (EB) and liposomes

1. For 2% EB dye solution, dissolve 1 g of EB in 50 mL of sterile saline. Filter the solution using 0.22 µm filters into

1.5 mL sterile tubes and store them at room temperature for later use.

2. For green-fluorescent liposomes, add POPC/Fl-DHPE (95:5), chloroform/methanol (2:1) into a 100 mL round bottom flask. Use a rotary evaporator at 150 rpm at 40 °C for 1 h, with vacuum maintained at 0 mbar[1] to create a thin lipid film.

   NOTE: When comparing effects of liposomal properties (e.g., size, charge, lipid saturation, lipid chain length) on distribution, maintain a fixed percentage of Fl-DHPE or other fluorescent lipids to confirm that the results observed are due to the effect of the properties tested, and not to the variable load of large hydrophobic dyes.

3. Hydrate the lipid film with phosphate-buffered saline (to achieve 26.3 mM of fluorescent liposomes) at 40 °C to form multi-lamellar vesicles (MLV). Load the MLVs into a glass syringe for manual extrusion (30 times using a 0.08 µm pore size polycarbonate filter) to achieve the desired size of 100 nm.

   NOTE: The temperature for hydration must be higher than the transition temperature of the lipids.

4. Filter the liposomes by passing them through a 0.22 µm sterile syringe filter. Confirm the hydrodynamic diameter (D_H) of the liposomes using a dynamic light scattering system.

2. Administration of EB and liposomes in live mice

1. Inject mouse with EB IV (intravenous) via the tail vein (2.5 mg/kg), 2 h before subconjunctival injection.

2. For subconjunctival injection, first, sedate the mouse using 5% isoflurane via inhalation in an induction chamber to achieve an adequate plane of anesthesia. Transfer the mouse to a nose cone and maintain sedation at 2%-2.5% of isoflurane while on a heating pad throughout the procedure.

3. Trim the whiskers near the eye to be injected and instill a drop of topical anesthetic 0.5% proxymetacaine hydrochloride solution directly on the eye.

4. Load a 10 µL glass syringe (with 32 G needle) with fluorescent liposomes (Fl-DHPE: 0.78 mg/kg) and dispel all air bubbles in the syringe prior to injection.

   NOTE: Up to 20 µL of injectate can be accommodated in the subconjunctival space of mice[18,19].

5. Using a tweezer, lift the conjunctiva slightly and inject slowly into the subconjunctival space (**Figure 1A**). Withdraw the needle slowly to prevent backflow. Ensure that a visible bleb filled with fluorescent liposomes is formed (**Figure 1C**).

6. Administer a drop of antibiotic 1% fusidic acid on the eye after the injection and monitor the mouse until it regains consciousness.

3. CLM set-up

1. Switch on the CLM system and make sure both the connector and the distal tip of the scanning probe are clean.

2. Clean the connector of the scanning probe using an optical connector cleaner by following the manufacturer's instructions.

   1. Press the rachet (often colored) of the optical connector cleaner to reveal a cleaning ribbon.

   2. Position the connector in contact with the cleaning ribbon and slide the connector along the ribbon while maintaining contact.

3. Clean the distal tip (also known as the scanning tip) of the probe by dipping it into the cleansing solution, followed by the rinsing solution provided by the manufacturer. A cotton tip applicator can also be used for more thorough cleaning if the tip is very dirty.

4. Connect the probe to the CLM system. Choose the Field of view (FOV) and the location for the acquisition files at this point.
   NOTE: Adjust the laser intensity at this step to ensure that fluorescence detection for FI-DHPE is in the linear range. Laser intensity is to be kept consistent for comparison between images taken at different time points.

5. Allow the system to warm up for 15 min as instructed and use the calibration kit to calibrate the system according to the manufacturer's instructions.
   NOTE: In the calibration kit, there are three vials for each laser containing the following solutions: cleansing solution, rinsing solution, and fluorophore 488/660 nm solution for internal calibration. The calibration steps are prompted by the system and are to be followed accordingly.
   1. Immerse the tip in the cleansing vial followed by the rinsing vial (5 s in each vial). Leave it in the air for background recording for both channels.
      NOTE: This step is very crucial as it normalizes the background values from different fibers of the probe and ensures image uniformity.
   2. Immerse the tip in the cleansing vial followed by the rinsing vial (5 s in each vial). Immerse the tip in fluorophore 488 nm vial for 5 seconds to normalize signal values from different fibers in the probe.
   3. Immerse the tip in the cleansing vial followed by the rinsing vial (5 s in each vial). Immerse the tip in the rinsing vial until the fluorescence signal recorded in 3.5.2. disappears. Immerse the tip in fluorophore 660 nm vial to normalize signal values from different fibers in the probe.
      NOTE: Follow all the calibration steps in order to achieve proper calibration and optimal image quality.

6. After calibrating the probe, check to make sure the background values for the probes are as low as possible. For the CLM system used, keep the background values below 100. Perform repeated cleaning of the probe with a cotton tip applicator and calibration if values are above 100/defined user value or if the probe appears to be dirty. This is to ensure that the background noise is kept around the same value.
   NOTE: It is important to define the maximum background value (for example, 100 as stated in step 3.6) to ensure that probe conditions are similar. This will allow proper quantitative comparison between images taken at different time points. The value may differ in different systems and probe conditions.

7. Switch on the animal temperature controller (ATC). Adjust the ATC to 37 °C. Cover the heating pad with a surgical drape and fix the nose cone on the heating pad.
   NOTE: ATC with an attached heating pad is required to ensure that the animal is kept warm throughout the imaging duration.

8. Clamp the stand of the dissecting microscope to the tabletop to secure it. Rotate and adjust the eyepiece of the microscope to view the mouse eye ergonomically through the eyepiece when the user is seated (make the adjustments after placing the animal).

9. Sedate the mouse using 5% isoflurane in an induction chamber. Transfer the mouse to the nose cone once the animal is non-responsive and maintain sedation at 2%-2.5% isoflurane while on a heating pad throughout the procedure.
10. Trim the whiskers of the mouse and instill a drop of anesthetic 0.5% proxymetacaine hydrochloride solution onto the eye.
11. To make sure the eyes are clean, drop a few drops of saline to wash the ocular surface.
12. Adjust the microscope so that the mouse eye is in direct focus at 0.67x magnification.
    NOTE: Make sure to lubricate the eyes with saline. If the eyes are not lubricated throughout the imaging session, they can get dry, causing the lens to crystallize. As a result, during CLM imaging, the lens can emit a background red fluorescence.

4. Live imaging of mouse eyes with CLM and acquisition

1. Turn on the laser, place the probe on the eye and start recording acquisition to observe the fluorescence in the eye at the regions indicated on the eye map in **Figure 3**.
   NOTE: Hold the probe like a pen with the distal end of the probe directly onto the region to be imaged.
2. Stop the recording when all regions have been flagged and labeled. The acquisition files will be saved automatically in the file location chosen in step 3.4.
   NOTE: The file will be saved as a video file which can be exported to individual images. Label the flag according to the eye map to know exactly the location of the probe at the exact frame the recording was done.

5. Image analysis

1. Using the same CLM acquisition software, export the image acquisition files for further analysis. Click on **File | Export** and choose the format to be exported to. Mkt format files will allow adjustments of look up table (LUT) and further exports to image file formats using the CLM viewer software.
2. For accurate comparison of fluorescence intensity, use the same LUT adjusted for each channel when exporting all image files.
   NOTE: Choose the minimum and maximum LUT threshold with respect to those of the control mouse (with no liposomes injected) to minimize background fluorescence readings.
3. Open the image in an appropriate image processing software/freeware program (e.g., ImageJ). Draw the region of interest (ROI).
   NOTE: ROI here refers to the region of interest in the processing program. In most cases, ROI will be the whole image scanned. However, in the case of imaging the limbus, the probe cannot just get the image of the limbus separately. Therefore, an ROI has to be drawn to 'quantify' the fluorescence in the limbus region, as drawn in **Figure 4**.To keep the ROI consistent, use the same ROI across all images.
4. Measure and record the ROI values for green fluorescence. Enter the values in a spreadsheet. Tabulate the average and fluorescence intensity (a.u.) values of the ROI.

6. Histology assessment

1. Euthanize the mouse using a method approved by the local IACUC.
2. Enucleate the eye and fix the eye in 1 mL of 4% formaldehyde or 10% formalin solution overnight.
3. Trim excess fats and embed the eye in the Optimal Cutting Temperature (OCT) compound and keep it frozen in a -80 °C freezer for at least one day.
4. Cut sections of 5 µm thickness in the cryostat with cutting temperature maintained at 20 °C. Transfer the section to a Poly-L-Lysine-coated microscope slide.
   NOTE: Histology can serve as additional validation of the distribution of DDS. However, it requires additional optimization, technical expertise, and sacrifice of animals which the study aims to reduce by using CLM.

Representative Results

The protocol demonstrates the utility of CLM to assess the spatio-temporal ocular distribution of green fluorescent liposomes administered through subconjunctival injection. To make use of the dual-color capability (488 nm and 660 nm excitation wavelengths) of the CLM system, 100 nm neutral POPC liposomes to be injected were doped with 5% FI-DHPE (composition and characterization data are shown in **Figure 1B**), and EB was injected IV to identify landmarks in the eye. The presence of a thin layer of episclera and the conjunctiva, which are both highly vascularized, allows the sclera region to be stained red with EB (**Figure 4A**, labeled as S), while the cornea which does not contain any vasculature (**Figure 4A**, labeled as C), does not get stained and appears black. This enables a distinct differentiation between both regions during fluorescence imaging.

The representative results are from a distribution study spanning over 7 days (n = 4 mice). As fluorescence intensities in the images for day 1 and day 3 were high (**Figure 5B**), the pixel intensities were reduced for better visualization. Actual values of the fluorescence intensity are reflected in the graphs (**Figure 6**). To ensure that observations from the images were due to fluorescence from the liposomes and not free dye, which might have dislodged from the liposomes, control mice injected with fluorescein (FI) dye was included (**Figure 5A**).

A reduction in the liposomes (by proxy of the decrease in green fluorescent signal) was observed in both the limbus and sclera regions over time. As the liposomes were injected from the temporal to the superior region of the subconjunctival space (**Figure 3**), they were naturally placed right on top of the temporal and superior sclera (**Figure 4B**) before reaching other regions of the subconjunctival space. On day 1 post-injection, fluorescence detected in the sclera was up to 6-times higher than the limbus for both temporal and superior regions (**Figure 6**). By day 3 and day 7, a significant reduction of liposomes was observed in the sclera (60% from day 1 to day 3 ($day_{1\rightarrow3}$) and 88% from day 3 to day 7 ($day_{3\rightarrow7}$)) in the temporal region, with a reduction of 66% and 93% for $day_{1\rightarrow3}$ and $day_{3\rightarrow7}$ in the superior regions, respectively, $p < 0.001$) (**Figure 6**). This reduction was attributed to the ocular clearance mechanisms through blood and/or lymphatic vessels found at the conjunctiva and episclera. The liposomes could also have diffused through the sclera and be cleared by the choroid, which is also highly vascularized.

The liposomes were found to have cleared in a slower manner in the limbus. For temporal limbus and superior limbus, the changes in fluorescence signals from day 1 to day 3 post-injection were not significant, indicating that neutral liposomes have a preference to the limbus region, particularly

the corneal periphery (**Figure 5B**). Liposomes in the limbus region started clearing from day 3 ($d_{3\rightarrow7}$: -89% for temporal ($p < 0.01$), and -53% for superior ($p < 0.05$)). By day 7, more than 90% of liposomes were cleared from all limbus regions ($p < 0.05$) except for superior limbus 1S, where 50% of liposomes could still be detected ($p > 0.05$). This is an indication that the residence time for neutral liposomes is much higher at the superior limbus/cornea periphery (**Figure 5** and **Figure 6**) when compared to other regions. The lowest amount of fluorescence was detected in the nasal and inferior regions at all time points due to their distance from the injection site (**Figure 6A**,**B**).

In more comprehensive studies of clearance of liposomes in the eye previously reported[1], we have discussed a few routes in which liposomes could be cleared from ocular tissues after subconjunctival injection. While liposomes can be cleared by systemic circulation and lymphatic clearance through the conjunctiva, episclera, and choroid, which are highly vascularized, they could also reach deeper intraocular tissues by passive diffusion through the sclera. Fluid flow could also transport the liposomes through the trabecular meshwork or uveosclera outflow, which can bring the liposomes back to the sclera. Elimination through tears is also possible, and minor leakages in the injection site could allow corneal penetration through passive diffusion.

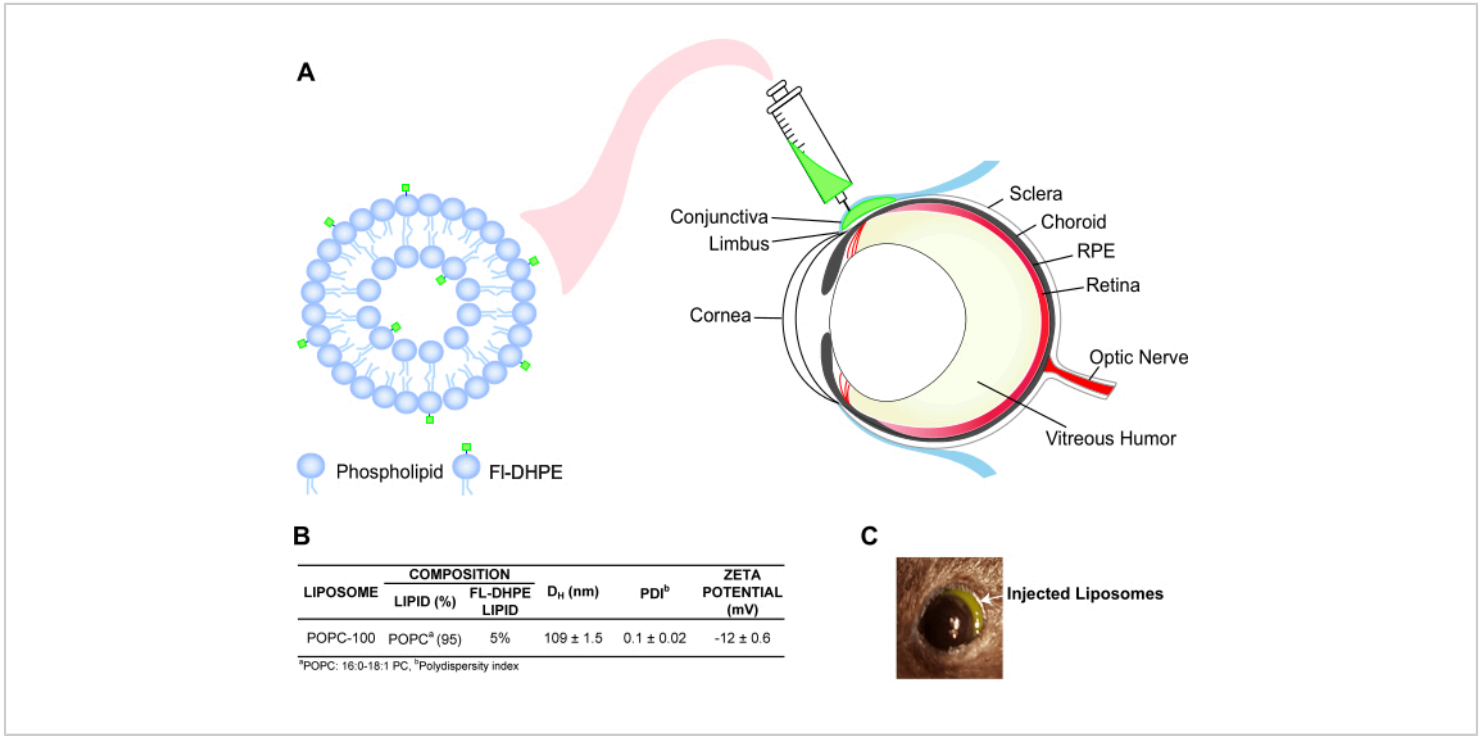

LIPOSOME	COMPOSITION		D_H (nm)	PDI[b]	ZETA POTENTIAL (mV)
	LIPID (%)	FL-DHPE LIPID			
POPC-100	POPC[a] (95)	5%	109 ± 1.5	0.1 ± 0.02	-12 ± 0.6

[a]POPC: 16:0-18:1 PC, [b]Polydispersity index

Figure 1: Subconjunctival injection of liposomes in the eye. (**A**) Graphical representation of green-fluorescent liposomes and subconjunctival injection. (**B**) Composition and properties of FL-DHPE doped liposomal formulation for ocular CLM Imaging. (**C**) Green-fluorescent liposomes forming a bleb upon subconjunctival injection. This figure has been adapted with permission from Chaw S.Y. et al.[1]. Please click here to view a larger version of this figure.

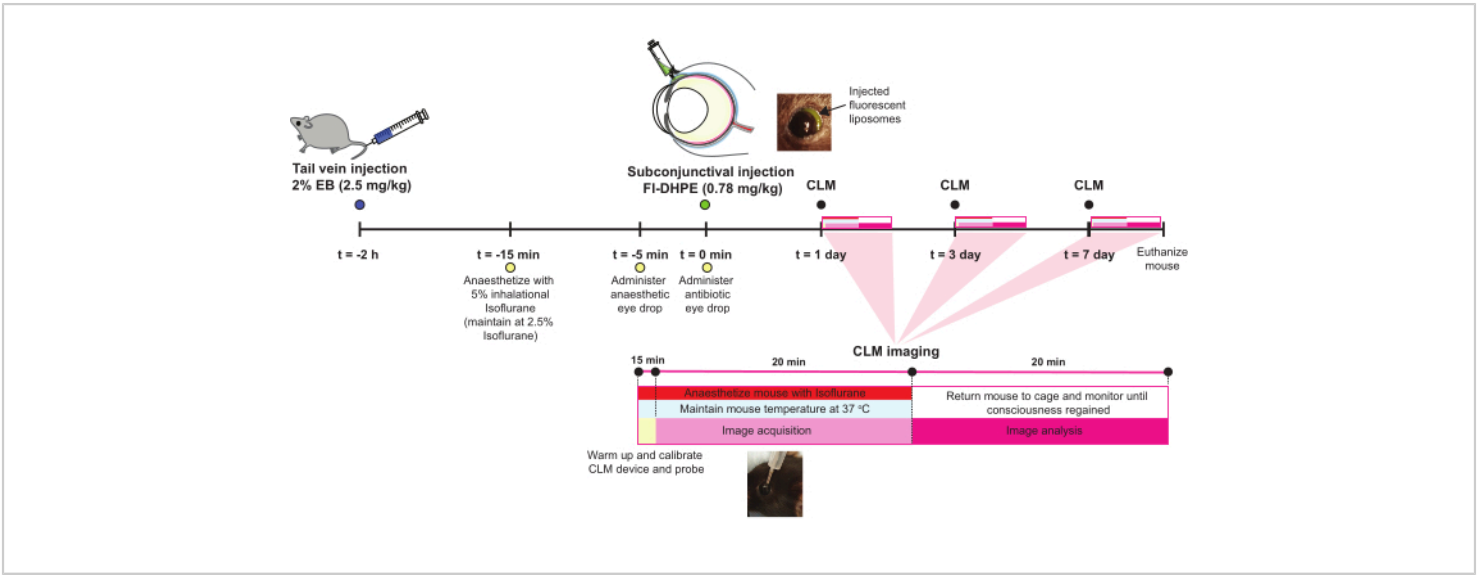

Figure 2: Timeline of ocular CLM procedure. Please click here to view a larger version of this figure.

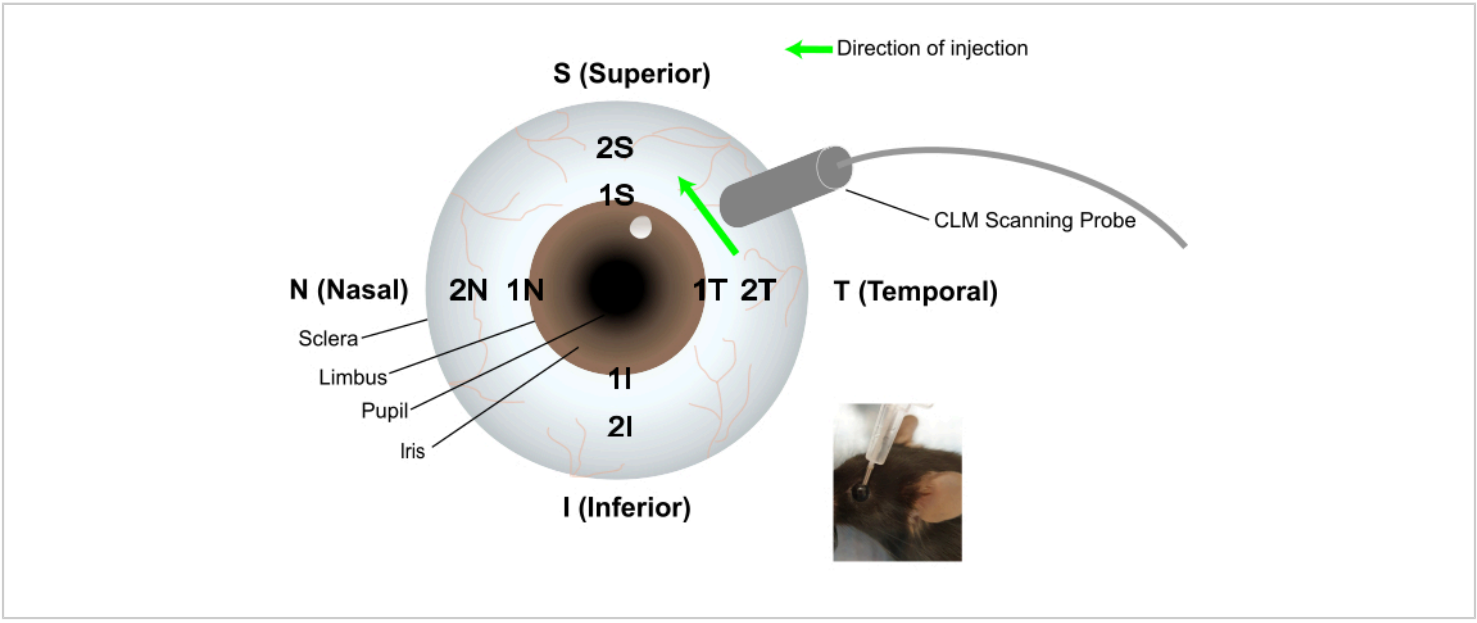

Figure 3: Eye map for CLM scans. Area 1 refers to the limbus region, while area 2 refers to the sclera region. Videos and images were taken from 1T in an anti-clockwise direction, followed by 2T in a similar anti-clockwise direction. As the needle was inserted for injection from 2T towards 2S, areas of interest are mainly 1T, 1S, 2T, and 2S. Insert shows the size of the probe relative to the mouse eye. This figure has been adapted with permission from Chaw S.Y. et al.[1]. Please click here to view a larger version of this figure.

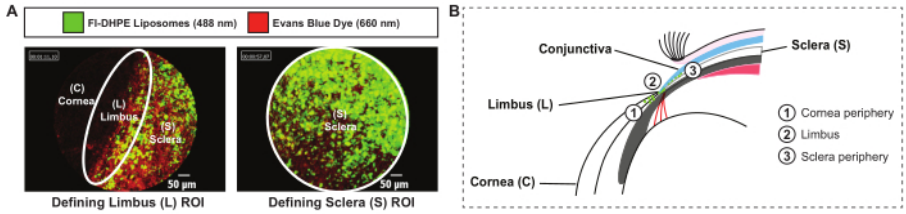

Figure 4: Image Analysis. (**A**) ImageJ analysis of fluorescent-tagged liposomes was done using regions of interest (ROI) defined for the limbus (L) and sclera (S) (**B**) Ocular regions quantified at the limbus region for liposome presence. Possible locations of liposomes detected in the limbus are 1) corneal periphery, 2) limbus or 3) sclera periphery. This figure has been adapted with permission from Chaw S.Y. et al.[1]. Please click here to view a larger version of this figure.

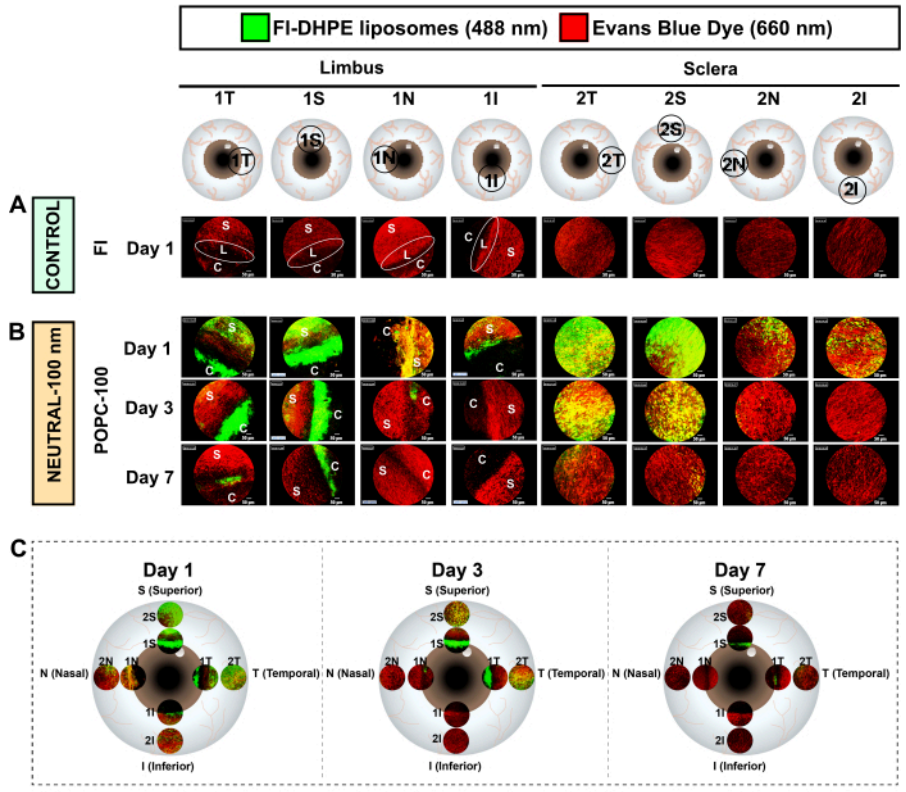

Figure 5: Contrast distributions at the limbus and sclera. Contrast distribution at the limbus (1S: Superior, 1N: Nasal, 1I: Inferior, 1T: Temporal) and sclera (2S: Superior, 2N: Nasal, 2I: Inferior, 2T: Temporal) regions of one representative mouse from each cohort (n=4) over 7 days for (**A**) Fluorescein (Fl) control, (**B**) 100 nm neutral liposomes (POPC-100). Red color indicates EB staining. Scale bar = 50 µm. (**C**) Images taken are assembled on the eye map for better understanding. This figure has been adapted with permission from Chaw S.Y. et al.[1]. Please click here to view a larger version of this figure.

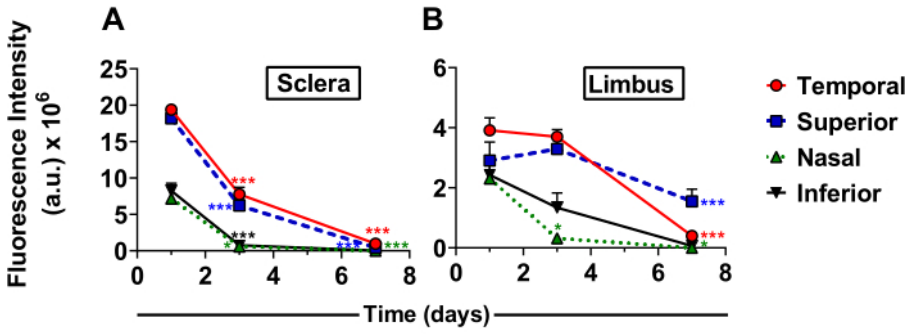

Figure 6: Clearance kinetics of 100 nm neutral POPC liposomes at the sclera (A) and limbus (B) regions over 7 days (n=4 mice per group). Mean fluorescence intensity was compared by 2-way ANOVA with multiple comparisons with respect to the previous time point; $d_{1\rightarrow3}$ and $d_{3\rightarrow7}$; *p < 0.05, **p < 0.01, ***p < 0.001. Please click here to view a larger version of this figure.

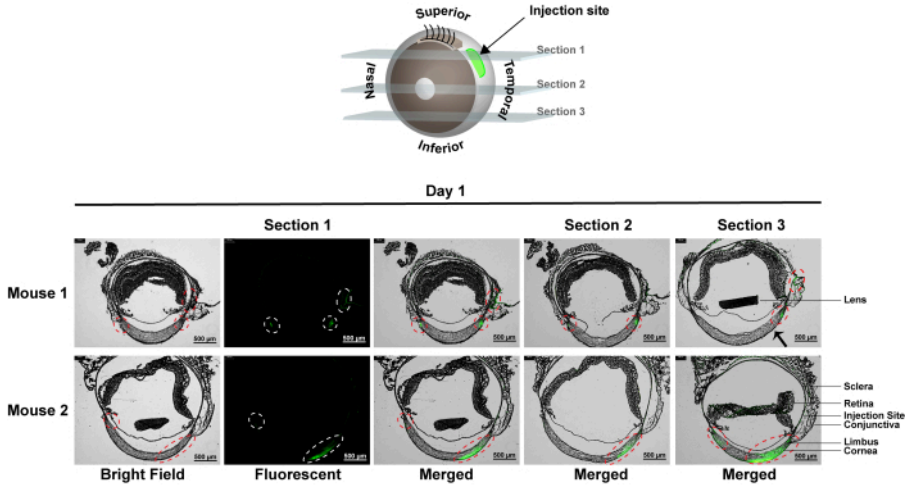

Figure 7: Representative histology images of transverse sections (5 µm) of mouse eye one day post-injection of FI-DHPE liposomes. Dotted lines indicate where the liposomes can be observed, indicated by green color. Scale bar = 500 µm. Please click here to view a larger version of this figure.

Discussion

As shown from the results, CLM provides a simple and feasible method to image the ocular distribution of liposomes in the eye. We previously demonstrated the use of CLM to characterize the localization of various liposomal formulations within the mouse eye over time[1]. For non-invasive applications, CLM permits real-time imaging of the anterior ocular surface for insights on how liposomes

are distributed in the eye from the same animal. This makes CLM suitable to pre-screen nanocarrier/DDS prior to more comprehensive quantification. Given the unique physiochemical properties of diverse DDS, it is rather challenging to characterize its sub-compartment distribution by conventional histology. The latter would require exhaustive sectioning of the whole eye and individual imaging sections by fluorescence microscopy for an overall sense of the DDS clearance.

In agreement with CLM images (**Figure 5B**,**C**), we could observe green fluorescent signals by histology at the cornea, limbus, and sclera regions of the eye collected at day 1 post-injection of the liposomes (**Figure 7**). Notably, CLM showed better sensitivity than fluorescent microscopy - liposomes at the sclera could be clearly detected using CLM (**Figure 5**) but barely detected by the fluorescence microscope (**Figure 7**). The signal loss could be due to the washing and sectioning procedures that affected the retention of liposomes in tissue sections. Although CLM is limited in pinpointing the exact tissue layer in which the liposomes accumulate, it is definitely a feasible and relatively straightforward method to screen and assess candidate ocular therapeutics non-invasively in real-time.

While other imaging systems like *in vivo* imaging systems and fluorometers also enable live imaging or live quantification of fluorescence in the eye, they are not as suitable for the purpose of this study. *In vivo* imaging systems do not offer the spatial resolution required to define where the therapeutics are in the ocular space. One can only get an idea of whether the therapeutics are still present in the ocular space and their biodistribution when using *in vivo* imaging system[20]. A fluorometer allows the measurement of fluorescence along the optical axis of the eye and is widely used to study physiological changes in the eye. As there is difficulty getting the exact same optical axis scanned at every time point, a consistent imaging spot cannot be maintained. This is very crucial, especially when studying the distribution of drug delivery systems in which their residence time and clearance rate from the injection site are totally unknown. Furthermore, the injection site and the distribution expected for subconjunctival injection are also not within the range of the optical axis.

Critical steps in the protocol include strictly following an imaging map similar to the eye map shown in **Figure 3** and labeling the locations accurately. Mis-labelling or deviation from imaging location would result in inconsistency of results. As laser intensity can be adjusted for each scan, it is important that the intensity is consistent for the quantification of different time points to be comparable. It is also important that the probe is kept free of debris during the imaging process. As eye mucus can get caught on the probe while imaging, rinsing the probe in saline is recommended if background values rise above the user-defined value.

Other than subconjunctival injection, this CLM system also has the potential to be used to study other ocular delivery routes such as eye drop administration and intravitreal injection (IVT). However, due to the limitation in imaging depth, it might not be as useful for IVT if the injection site and deeper ocular tissues are the main areas of interest. CLM can also be used as a form of intravital imaging to study the distribution of DDS in other organs or tissues. Although it has rarely been employed to study DDS distribution, endoscopic confocal microscopy has been used to image inflammation caused by periodontitis[21], monitor pulmonary inflammation and infections[22,23] and effect of drugs on angiogenesis in

tumors[24], indicating a range of other possible applications for this CLM system.

Overall, this protocol could serve as a screening step to find out how modifications in DDS formulations affect where they reside or accumulate, which could be critical in the design of a DDS.

Disclosures

The authors have nothing to disclose.

Acknowledgments

This research was funded by NTU-Northwestern Institute for Nanomedicine (NNIN) grant awarded (to SV) and in part by Singapore National Research Foundation Grant AG/CIV/GC70-C/NRF/2013/2 and Singapore's Health and Biomedical Sciences (HBMS) Industry Alignment Fund Pre-Positioning (IAF-PP) grant H18/01/a0/018 administered by the Agency for Science, Technology and Research (A*STAR) (to AMC). Thanks to members from Duke-NUS Laboratory for Translational and Molecular Imaging (LTMI) for facilitating the logistics and execution of the studies and training on equipment. Special thanks to Ms. Wisna Novera for her editorial assistance.

References

1. Chaw, S. Y., Novera, W., Chacko, A.-M., Wong, T. T. L., Venkatraman, S. *In vivo* fate of liposomes after subconjunctival ocular delivery. *Journal of Controlled Release.* **329**, 162-174 (2021).
2. Kuo, J. C.-H. et al. Detection of colorectal dysplasia using fluorescently labelled lectins. *Scientific Reports.* **6** (1), 24231 (2016).
3. Wu, Y.-F. et al. A custom multiphoton microscopy platform for live imaging of mouse cornea and conjunctiva. *Journal of Visualized Experiments: JoVE.* **159**, e60944 (2020).
4. Zhivov, A., Stachs, O., Kraak, R., Stave, J., Guthoff, R. F. *In vivo* confocal microscopy of the ocular surface. *The Ocular Surface.* **4** (2), 81-93 (2006).
5. Bassyouni, F., ElHalwany, N., Abdel Rehim, M., Neyfeh, M. Advances and new technologies applied in controlled drug delivery system. *Research on Chemical Intermediates.* **41** (4), 2165-2200 (2015).
6. Sercombe, L. et al. Advances and challenges of liposome assisted drug delivery. *Frontiers in Pharmacology.* **6**, (2015).
7. Koning, G. A., Storm, G. Targeted drug delivery systems for the intracellular delivery of macromolecular drugs. *Drug Discovery Today.* **8** (11), 482-483 (2003).
8. Metselaar, J. M., Storm, G. Liposomes in the treatment of inflammatory disorders. *Expert Opinion on Drug Delivery.* **2** (3), 465-476 (2005).
9. Ding, B. S., Dziubla, T., Shuvaev, V. V., Muro, S., Muzykantov, V. R. Advanced drug delivery systems that target the vascular endothelium. *Molecular Interventions.* **6** (2), 98-112, (2006).
10. Hua, S., Wu, S. Y. The use of lipid-based nanocarriers for targeted pain therapies. *Frontiers in Pharmacology.* **4**, 143 (2013).
11. Sharma, A., Sharma, U. S. Liposomes in drug delivery: Progress and limitations. *International Journal of Pharmaceutics.* **154** (2), 123-140 (1997).
12. Abrishami, M. M. et al. Preparation, characterization, and *in vivo* evaluation of nanoliposomes-encapsulated

Bevacizumab (Avastin) for intravitreal administration. *Retina.* **29** (5), 699-703 (2009).

13. Pleyer, U. et al. Ocular absorption of cyclosporine A from liposomes incorporated into collagen shields. *Current Eye Research.* **13** (3), 177-181 (1994).
14. Shen, Y., Tu, J. Preparation and ocular pharmacokinetics of ganciclovir liposomes. *The AAPS Journal.* **9** (3), E371-E377 (2007).
15. Weijtens, O. et al. High concentration of dexamethasone in aqueous and vitreous after subconjunctival injection. *American Journal of Ophthalmology.* **128** (2), 192-197 (1999).
16. Voss, K. et al. Development of a novel injectable drug delivery system for subconjunctival glaucoma treatment. *Journal of Controlled Release.* **214**, 1-11 (2015).
17. Giarmoukakis, A. et al. Biodegradable nanoparticles for controlled subconjunctival delivery of latanoprost acid: *In vitro* and *in vivo* evaluation. Preliminary results. *Experimental Eye Research.* **112,** 29-36 (2013).
18. Shah, N. V. et al. Intravitreal and subconjunctival melphalan for retinoblastoma in transgenic mice. *Journal of Ophthalmology.* **2014**, 829879 (2014).
19. Dastjerdi, M. H., Sadrai, Z., Saban, D. R., Zhang, Q., & Dana, R. Corneal Penetration of Topical and Subconjunctival Bevacizumab. *Investigative ophthalmology & visual science.* **52** (12), 8718-8723 (2011).
20. Ezra-Elia, R. et al. Can an *in vivo* imaging system be used to determine localization and biodistribution of AAV5-mediated gene expression following subretinal and intravitreal delivery in mice? *Experimental Eye Research.* **176**, 227-234 (2018).
21. Movila, A. et al. Intravital endoscopic technology for real-time monitoring of inflammation caused in experimental periodontitis. *Journal of Immunological Methods.* **457**, 26-29 (2018).
22. Vanherp, L. et al. Bronchoscopic fibered confocal fluorescence microscopy for longitudinal *in vivo* assessment of pulmonary fungal infections in free-breathing mice. *Scientific Reports.* **8** (1), 3009 (2018).
23. Chagnon, F. et al. *In vivo* intravital endoscopic confocal fluorescence microscopy of normal and acutely injured rat lungs. *Laboratory Investigation.* **90** (6), 824-834 (2010).
24. Yun, J. Y. et al. The effect of near-infrared fluorescence conjugation on the anti-cancer potential of cetuximab. *Laboratory Animal Research.* **34** (1), 30-36 (2018).